Investigation of the Nonlinear Refractive Index of MCF7 and MCF10A Breast Cell Lines for Optical Diagnosis

Bahareh Khaksar Jalali [a, b, *], Somayeh Salmani Shik [a, c], Latifeh Karimzadeh Bardeei [d], Sharife Shahi [b, e,*]

[a] Department of physics, Kharazmi University, Tehran, Iran.
[b] Laser and Biophotonics in Biotechnologies Research Center, Islamic Azad University of Isfahan (Khorasgan) branch, Isfahan, Iran.
[c] Applied Sciences Research Center, Kharazmi University, Karaj, Iran.
[d] Department of animal biology, Faculty of biological sciences, kharazmi university, Tehran, Iran.
[e] Department of Biomedical Engineering, Islamic Azad University of Isfahan (Khorasgan) branch, Isfahan, Iran.

***Coressponding author: biophotonics.bkhj@gmail.com**
***Coressponding author: shahilaser@khuisf.ac.ir**

Received: Oct. 12, 2022, Revised: Jan. 3, 2023, Accepted: Jan. 31, 2023, Available Online: Feb. 14, 2023
DOI: 10.30495/ijbbe.2023.1969265.1016

ABSTRACT: To demonstrate that the Z-scan technique is a reliable approach for diagnosing normal and cancer cells, the absorption coefficient (α), nonlinear refractive index (n2) of normal (MCF10A) and cancer cell lines (MCF7) were examined. According to our findings of the optical properties of cells, cancer cells shown to have higher linear absorption coefficient than normal cells as well as nonlinear refractive index (n2) of different signs but the same order of (10-7 cm2/W). This method is a quick method for differentiating between normal and cancerous breast cells, making it suitable for use in clinical stages in the future. This is because of the obvious fundamental difference between the optical behavior of normal and cancer cells, as well as the affordability, the potential for reproducibility without compromising sample quality, and the high accuracy.

KEYWORDS: Cancer Diagnosis, Linear Absorption, MCF7, MCF10A, Optical Coefficients, Z-scan Technique.

I. INTRODUCTION

Today, no one is unaware of the biology behind a common illness like cancer. In order to improve and increase the effectiveness of therapies, there has to be more information and study in this area [1]. This will lead to a precise, efficient, and early diagnosis of cancer as one of the highly widespread illnesses. The known causes of cancer consist a number of factors, including environmental elements, inherited traits, and gene abnormalities resulting in mutations [2]. Female breast cancer, lung cancer, and prostate cancer are the most commonly diagnosed cancers worldwide, according to the International Agency for Research on Cancer (IARC) GLOBOCAN. The information is based on collected statistical data from population based cancer registries (PBCRs) and the World Health Organization (WHO 2020) [3]. Furthermore, after lung cancer, breast cancer is the second greatest cause of cancer death in women population [4]. As a result, prevention, early detection, and high-quality therapy can help minimize cancer deaths [5].

Many ways have been proposed, including the use of lasers and the investigation of the optical behavior of materials for diagnosis and treatment [6, 7], because the analysis of the

optical interaction between the laser beam and the tissue leads to a wide range of applications [8].

The accuracy of the diagnosis is crucial for determination of the best course of therapy, and thus lowering the mortality of the cancer disaster [9, 10]. As a result, diagnosis is of particular relevance in today's cancer research. One frequent technique for detecting breast cancer is the examination of chromatin interactions at the genome level. This approach is suggested because each chromosome is referenced to a specific location within the nucleus that might not be always be stable. This is due to the fact that the chromosomes with dense genes typically stay in the nucleus, whereas gene-poor chromosomes are found close to the nucleus' periphery. In addition, HER2 (human epidermal growth factor receptor 2) protein status can be determined using the immunohistochemistry (IHC) technique. By examining the correlation between HER2 status and morphological characteristics, chromogenic in situ-hybridization (CISH) and fluorescence in situ-hybridization (FISH) of HER2 variations are used to assess gene amplification. However, all of these procedures are time consuming, and cost incurring procedures [11-13]. As a result, it seems ideal to have an accurate, quick, and low-cost diagnostic approach for all forms of cancer.

The Z-scan technique, developed by Sheikh Baha'i et al. in 1990 for assessing nonlinear optical characteristics, is one of the most exact, practical, and dependable optical techniques utilized in biomedical diagnostics method today [14]. This optical method has been demonstrated to be a sensitive technique for quantifying a wide range of LDL (low-density lipoprotein) values. The nonlinear optical response is influenced by different fractions of LDL, such as free and esterified cholesterol, triglycerides, fatty acids, and phospholipids. The phospholipid molecules from the outer shell, of course, appear to be the principal contributors to the nonlinear optical observations on LDL. Because LDL does not exhibit a Z-scan signal, the oxidation process has significantly affected this fraction of LDL, affecting the size of the nonlinear response. The amplitude of the nonlinear response of LDL particles, on the other hand, increases with temperature. These findings suggest that this method could be used as a spectroscopic tool to analyses the structure of LDL. Another method of diagnosing heart disease was proposed in 2006 by analysing the thermal nonlinear optical response of human normal and copper-oxidized low-density lipoproteins (LDLs). In this method the Z-scan technique was used as a function of temperature and LDL particle concentration for analysis. This method permits the detection of changes related to inflammatory stress and can thus indirectly measure the stability and susceptibility of LDL, associated to the presence of heart disease [15]. The amplitude of the Z-scan signal as a function of the LDL concentration showed a linear behavior considering the Beer-Lambert law [16]. In 2010, Dhinaa and Palanisamy used the Z-scan approach with 532 nm Nd:YAG CW and 633 nm He-Ne lasers to measure total protein and albumin. Their findings exactly matched those of the traditional colorimetric method. Additionally, they demonstrated in the other study that the 532 nm Nd:YAG CW method provided adequate results in comparison to the traditional colorimetric method for displaying the nonlinear optical properties of some other bioanalytes, such as urea and uric acid in the blood samples [17, 18].

Creatinine levels in the blood rise as a result of renal cleansing failing. Renal problems are more likely to occur with an increase in creatinine. Renal failure is always evaluated by measuring the blood creatinine level using conventional methods, the Jaffe technique, and enzymatic procedures. Ghader et al. made the first nonlinear refractive index calculation of the plasma creatinine levels in humans. They demonstrated that their results had sufficient precision and were equivalent to the conventional Jaffe approach when they were repeated numerous times [19]. Ghader et al. (2018) looked at the possibility of the Z-scan approach as a highly accurate, low-cost, and quick diagnostic optical technique to define abnormalities in two different breast cancer cell

lines, SK-BR-3 and MCF7. They claimed that each cell line with distinct nonlinear refractive index can be used as a marker to distinguish various breast cell lines [20]. Also, certain validated data from the Majles ara's research group considering the application of the Z-scan for early diagnosis of selected human brain (U87MG) and breast (mda-mb-231) malignant tumor cells were published in 2019. This study shows the compatibility of the obtained results with the previous findings [21, 22].

In this study, a very precise and repeatable diagnostic method for distinguishing between healthy breast cells and cancer cells was provided. Despite the fact that MCF10A and MCF7 are both epithelial, we have been able to provide a detection method for normal and abnormal cell conditions. In this regard, a higher background interaction frequency has been detected in the MCF7 genome compared to the MCF10A. This may be due to an increase in the variety of interactions within the genome. Higher-order chromatin structure is disrupted in cancer cells. The intra-chromosomal connections between breast cancer cells and breast epithelial cell types varied significantly as well. Additionally, due to the structural variations, some elasticity or subcellular structures developed [23, 24]. MCF10A breast epithelial cells are classified as normal cells and non-tumorigenic, and MCF7 is the malignant breast epithelial cell line [25, 27]. The objective of this study is to evaluate the optical characteristics of cells in order to make a non-invasive in-vitro distinction between breast cancer cells and the matching normal cells.

II. MATERIAL AND METHODS

A. *Sample preparation*

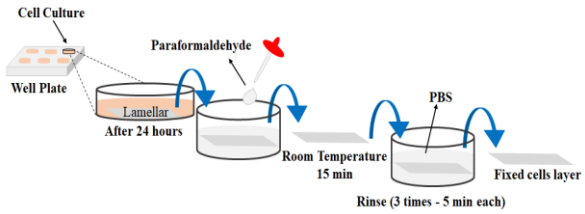

Fig. **1** Preparation of transparent samples by fixing cells on lamellar.

Iranian Biological Resource Center provided the human mammary cell lines MCF7 and MCF10A. They were cultivated in individual cell culture flasks with Dulbecco's Modified Eagle's medium (DMEM-Gibco), 10% fetal bovine serum (FBS-Gibco), 100 units/ml penicillin, and 100 µg/ml streptomycin antibiotic (Sigma-Aldrich), with DMEM culture medium at 37°C in an incubator with 5% CO2. Each cell line was given its own plate with six wells, into which a sterile layer was inserted. Following cell counting, 10×10^3 cells were added to each well and cultured for 24 hours to allow for cell growth, proliferation, and adherence to the slide. The samples were then submerged in a 1 ml solution of 4% paraformaldehyde. After leaving the solution, the layers were allowed to cool for 15 minutes at ambient temperature. Finally, the samples were washed three times with PBS for 5 minutes each before being transferred in fixed form to the optical apparatus shown in **Figs. 2** and **3**. **Fig. 1** depicts the full stabilizing procedure.

B. *Fundamental of optical method*

1) Measurement of linear absorption

The 532 nm Nd:YAG laser is put in a basic optical setup (see Fig. 2) to investigate the linear absorption coefficient in Eq (1).

$$S = 1 - exp\left(\frac{-2r_a^2}{w_a^2}\right) \quad (1)$$

In this equation, I_0 , L and α are, initial intensity, the length of sample, and the linear absorption coefficient of sample, respectively. According to this relation, the absorption coefficient depends on the intensity of the incident beam, path length, concentration of the absorbing species (chromophores) and the extinction coefficient [28].

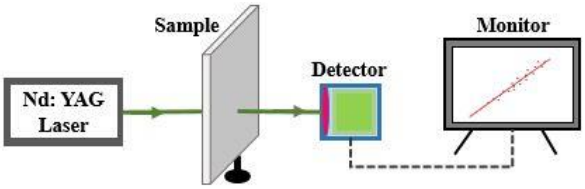

Fig. **2** Schematic of optical setup to investigate linear absorption coefficient of fixed layers of cell lines.

2) Closed-aperture Z-scan setup

Figure 3 depicts the schematic diagram of the closed-aperture optical Z-scan. The approach is used to determine the sign and magnitude of a material's nonlinear refractive index (here cell layers; biomaterials). The focused laser beam impinges upon the sample by passing through the aperture centered on the beam's axis. The strength of the incident beam varies as the sample moves across the Z-axis around the focal point from -Z to +Z. This tendency may produce a change in the material's refractive index, resulting in a change in the beam radius over the aperture plane. As a result, the transmitted laser beam can be used to calculate the nonlinear refractive index of any material.

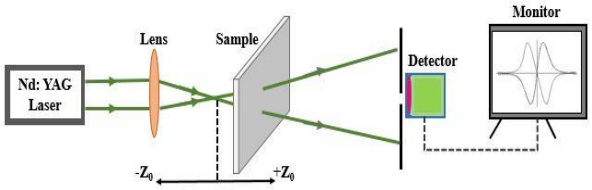

Fig. **3** Schematic of experimental closed-aperture Z-scan setup.

A 532 nm Nd:YAG laser with a maximum output power of 110 mW was employed as the coherent light source in this optical system [20, 29, 31]. The laser light has a beam width of 44 m and is focused through an 80 mm focal length lens. This beam passes through a nonlinear sample, causing a change in the overall refractive index proportional to the intensity of the beam and the material's nonlinear optical behaviour. In the simplest case, under the third-order nonlinearities condition, this leads to the change $n = n_0 + n_2 I$ [32], where n, n_0, n_2, and I are total refractive index, linear refractive index, the third-order nonlinear refractive index, and incident intensity, respectively. The intensity of the incident laser beam with a Gaussian profile creates a nonlinear refractive index in the sample, causing it to operate as a positive or negative lens to change the wave-front, a phenomenon known as self-focusing and self-defocusing nonlinear optical phenomena [33].

These modifications can be estimated using n_2 and Eq. (2): $n_2 = \dfrac{\lambda \Delta T_{P-V}}{2\pi L_{eff}\,(0.406)(1-S)^{0.25} I_0}$

In this relation , λ, ΔT_{P-V}, L_{eff}, and I_0 are the wavelength of the laser beam, the difference between maximum (peak) and minimum (valley) of the normalized transmittance power, the effective length of sample, and the maximum intensity at the focal point, respectively [34]. In addition, S is linear transmittance of the aperture calculated by **Eq. (3)**; r_a is its radius and w_a is the Gaussian beam radius on the aperture plate.

$$S = 1 - exp\left(\frac{-2r_a^2}{w_a^2}\right) \tag{3}$$

I_0 can be calculated by **Eq. (4)**, where w_0 and P are the beam waist and input power, respectively. The L_{eff} value is also determined by **Eq. (5)**, α is the linear absorption coefficient and L is the sample length.

$$I_0 = \frac{2P}{\pi w_0^2} \tag{4}$$

$$L_{eff} = \frac{1 - e^{-\alpha L}}{\alpha} \tag{5}$$

It is noteworthy that in the closed-aperture Z-scan curve, the sign of n_2 is negative when the transmission peak is observed before the valley, and this parameter would be positive when the transmission peak comes after the valley [14], [34].

III. RESULT AND DISCUSSION

In this paper, eight samples were divided into two major biological layer groups where MCF10A refers to normal breast cells, while MCF7 is cancer breast cells. To increase the accuracy of the results, each group contains four separate samples, and all data analysis has been repeated three times at different parts of each layer. Because of the variation of the cell arrangement all final obtained results from the data analysis will have averages values. In many circumstances, cell samples cannot be examined immediately after collection and must be fixed using chemical procedures. Fixation not only inhibits cell autolysis, but also retains all cell components, cell morphology and structural integrity, and thus enhances the microscopic appearance of cells. Also, by doing so, the essential chemical and physical properties of the cells is maintained. One of the most commonly utilised chemical agents for cell samples is paraformaldehyde (PFA). PFA creates covalent cross-links between molecules, thereby bonding them into an insoluble meshwork. However, investigations have demonstrated that fixation at 4% corresponds to optimum cell fixation in biological protocols, and fixation in protein cross-linking reagents like paraformaldehyde retains cell structure better than organic solvents [35, 36]. Notably, no paraformaldehyde solution, PBS solution, culture medium, or lamellar slide exhibited nonlinearity. As a result, all nonlinear reactions are caused by cellular activities. **Fig. 4** depicts transmission measurements of MCF10A and MCF7 bio-layers exposed to a low-power laser at 532 nm. These samples' linear absorption coefficients (α) were computed using a 1 mm sample length and the slope of each line. **Table 1** shows the linear absorption coefficients (α) of all samples and the mean of both cell lines. Cancer cells are obviously stronger attenuators than normal cell lines since their linear absorption coefficient (α) is substantially higher [37].

Table **1** Linear absorption coefficient values of all MCF10A and MCF7 samples and average values assigned to each cell line.

Cell line	Sample number	Linear absorption coefficient (α), (cm^{-1})	
MCF10A	1	1.58	Mean
	2	1.65	
	3	1.83	1.8
	4	2.14	
MCF7	1	3.45	
	2	3.62	
	3	3.67	3.66
	4	3.81	

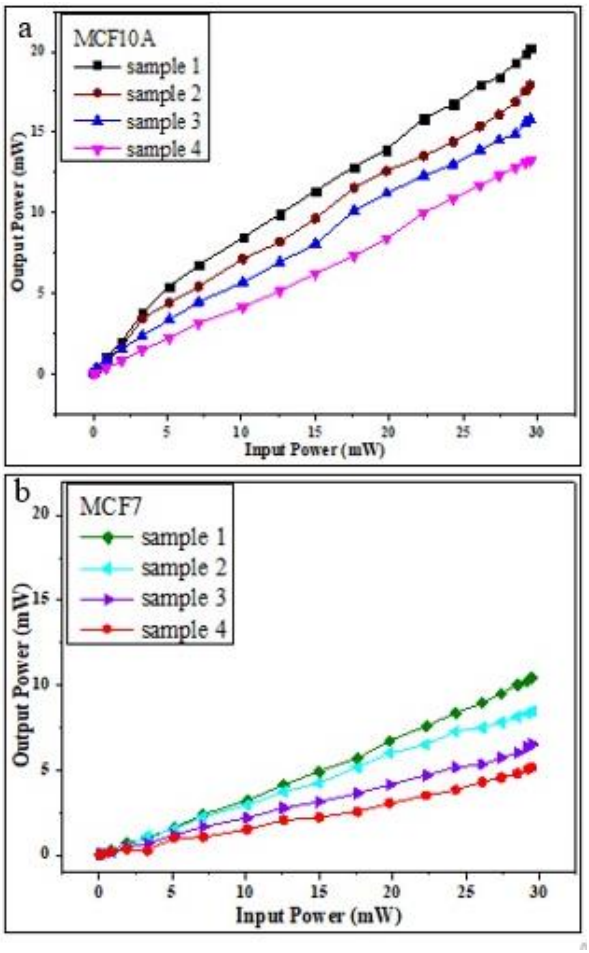

Fig. **4** Linear absorption coefficient (α) for 8 samples. a) MCF10A, b) MCF7 cell lines.

The nonlinear refractive index (n_2), which is measured using the close-aperture Z-scan technique, is one of the third-order nonlinear coefficients. All samples were used in the arrangement illustrated in **Fig. 3** to test their nonlinear optical properties. **Fig. 5** depicts all of the nonlinear refractive indices of the MCF10A and MCF7 layers. The sign of n_2 is

positive for all MCF10A cell lines, where the cells behave like a convex lens, which is known as self-focusing. The sign of the nonlinear refractive index of all MCF7 layers are negative, similar to a concave lens. This process is known as self-defocusing. **Table 2** shows the nonlinear refractive index values for all samples. These cell lines show considerable genome-wide interaction differences, with MCF10A showing a strong physical closeness of gene-rich, with tiny chromosomes (chr16-22) compared to MCF7. As a result, there is a considerable rise in inter-chromosomal connections between chr16 and chr22 in the MCF10A genome; this region contains the most gene-dense chromosomes in the human genome. According to research, the interaction frequency of tiny and gene-rich chromosomes chr16 through chr22 in MCF7 breast cancer genome representation is lower than in MCF10A epithelial cells, which is connected with the presence of more open components in MCF7 chr16-22. Furthermore, structural changes dictate the unique elasticity of whole cells with subcellular structures, implying that the individual tumor cells are roughly twice as soft as normal tissue cells. These changes in elasticity between normal and tumor cells are caused by variances in the size of the actin cortex linked to the cellular membrane, the makeup of the cytoskeleton, and varying levels of nuclear proteins. MCF7 cells are larger and have very poor cytoplasm and nucleus flexibility (based on Young's modulus) than normal MCF10A breast cells [23, 24]. Actin is a relatively abundant intracellular protein that plays an important functional role in determining cell shape and structure, hence modulating tensions locally. As a result, the diameter of the actin cortex of MCF7 cancer cells is clearly smaller than that of MCF10A normal cells [38]. **Table 3** contains a list of these parameters. The nonlinear refractive index of the cell environment will be altered as a result of the biological changes that have occurred in the structure of normal and malignant cells. These modifications will also result in nonlinear optical effects such as self-focusing and self-defocusing.

Table **2** Nonlinear refractive index values of all MCF10A and MCF7 samples and average values assigned to each cell line.

Cell line	Sample number	Nonlinear Refractive Index ($n_2 \times 10^{-7}$ cm^2/W)	
MCF10A	1	+ 4.68	Mean
	2	+ 4.77	+ 4.79
	3	+ 4.84	
	4	+ 4.89	
MCF7	1	- 9.71	
	2	- 9.76	- 9.78
	3	- 9.82	
	4	- 9.86	

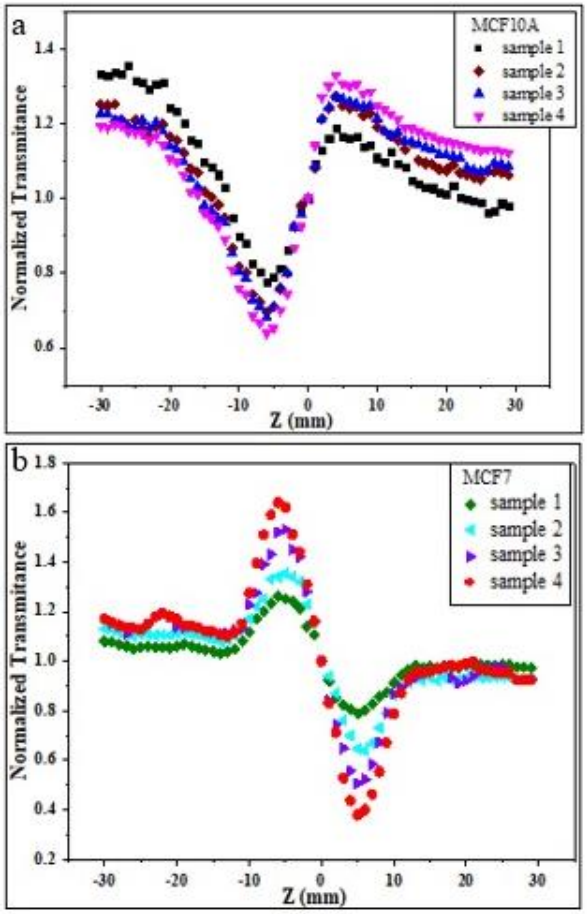

Fig. **5** Normalized data of Close aperture Z-scan (n_2) for 8 samples. a) MCF10A cell line, b) MCF7 cell line.

The trend of the optical behavior of the cells with respect to each other is visualized in **Fig. 6**, which is based on the average values of the samples. As can be seen, the linear absorption coefficients differ greatly. Furthermore, **Fig. 6.b**. clearly illustrates that the nonlinear refractive index has the potential to differentiate cancer cells from healthy cells, as the signs of these parameters differ, as shown + 4.79 × 10^{-7}

cm^2/W for MCF10A and - 9.78×10^{-7} cm^2/W for MCF7 cells.

Table **3** Different dynamic parameters of normal MCF10A normal breast cells and MCF7 cancer breast cells [23].

Parameter / unit	MCF7	MCF10A
Cell volume / μm^3	3375 - 16873	678 - 1317
Cytoplasm Young's modulus / kPa	0.47	0.7
Nucleus Young's modulus / kPa	4.7	7
Actin cortex diameter / μm	1.27 – 2.17 (13.5%)	1.37 – 2.47 (20%)

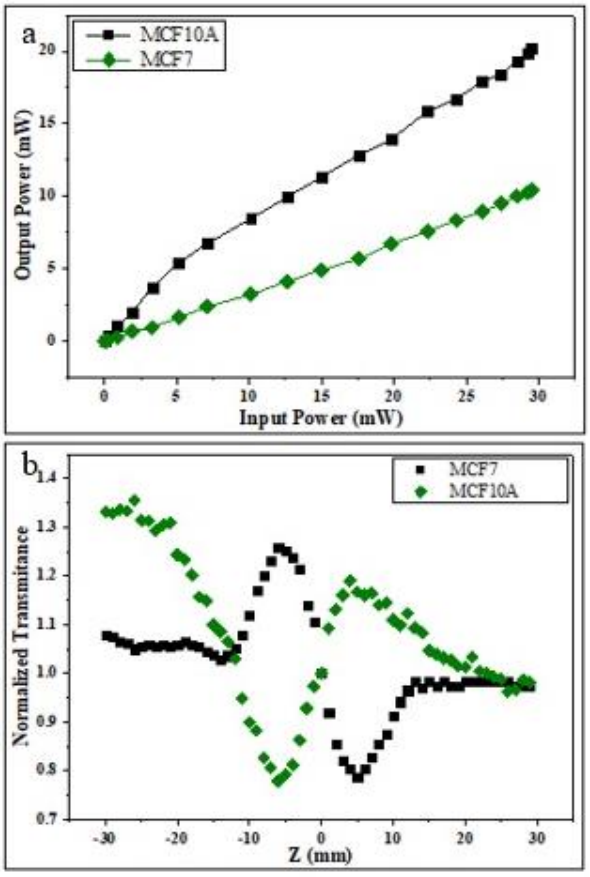

Fig. 6 Comparative optical behavior of MCF10A and MCF7 cells. a) Linear absorption coefficients (α), b) Nonlinear refractive index (n_2).

The nonlinear optical behavior of normal and cancerous human cells was studied in 2016 for cancerous ovarian cells using the Z-scan technique on the order of 10-8 (cm2/W) [39]. Another study of benign and malignant brain tissue in 2018 showed that the mean nonlinear refractive index for each tissue was on the order of 10^{-5} (cm^2/W) with having opposite signs [29].

The nonlinear refractive index of the U87MG brain cell line is estimated to be on the order of 10^{-7} (cm^2/W) [21]. The nonlinear refractive index of the mda-mb-231 cell line is 1.83×10^{-7} (cm^2/W) [22], whereas the SK-BR-3 and MCF7 cells had nonlinear refractive indexes of 18.14×10^{-7} and - 9.73×10^{-7} (cm^2/W), respectively [20]. In comparison to the current investigation, the order and sign of the nonlinear refractive index for the MCF7 cancer cell are close to (- 9.78×10^{-7} (cm^2/W)). As a result, it appears that in the optical method of cancer diagnostic tests, the varied signs and the order of the distinct cell lines are more essential than the value of the nonlinear refractive index. These results suggest that the optical approach is not only reliable for discriminating between normal and malignant cell lines, but it can also differentiate the different cell lines by a specific amount of nonlinear refractive index, for example with n_2 for breast cell lines being around 10^{-7} (cm^2/W). Aside from that, this approach can be used to diagnose and distinguish any type of the cell, including cancer cells (brain or breast in this case). Because of the local metabolic and structural changes that occur at the cellular and subcellular levels of malignant tissue, such as changes in chemical components, cell size, and shape, that are likely to affect the optical properties of the tissue, such as scattering, absorption, and fluorescence. It is important to mention that hemoglobin, melanin, proteins, DNA, genetic variations, and dynamic changes can also affect the light absorption, and scattering properties [23, 29]. In this case the samples can also be reused due to the fact that PBS protects samples and Nd:YAG laser have no longer any destructive effect. Finally, since this method is simple, affordable, and non-time-consuming, thus the cells under consideration will survive the irradiation [40].

IV. CONCLUSION

In conclusion, nonlinear optical behavior can be seen in both healthy and cancerous breast cells. Despite the fact that all samples have nonlinear refractive indices of the same order (10^{-7}

cm^2/W), MCF10A and MCF7 have opposite signs. MCF10A bio-layers exhibit self-focusing behavior, whereas MCF7 bio-layers exhibit self-defocusing behavior. The optical behavior might help distinguish between MCF7 and MCF10A. It might be a means of assessing the nonlinear optical qualities in future medical diagnosis. Because nonlinear activity is more accurate than linear one when it comes to identifying healthy cells. Additionally, this straightforward procedure can be used again without affecting the samples' characteristics. The interactions between the the laser and the materials (in this case, the cells) expose the material's optical properties, and thus making this as a crucial parameter in nonlinear optics.

REFERENCES

[1] M. Ravikumar and P. G. Rachana, "Study on Different Approaches for Breast Cancer Detection: A Review," SN Comput. Sci. vol. 3, no. 1, pp. 1–6, 2022.

[2] K. Czene, P. Lichtenstein, and K. Hemminki, "Environmental and heritable causes of cancer among 9.6 million individuals in the Swedish family-cancer database," Int. J. cancer, vol. 99, no. 2, pp. 260–266, 2002.

[3] J. Ferlay, M. Colombet, I. Soerjomataram , D. M Parkin, M. Piñeros, A. Znaor, and F. Bray, "Cancer statistics for the year 2020: An overview," Int. J. cancer, vol. 149, no. 4, pp. 778–789, 2021.

[4] C. E. DeSantis, J. Ma, M. M. Gaudet, L. A Newman, K. D Miller, A. Goding Sauer, A. Jemal, and R. L Siegel , "Breast cancer statistics, 2019," CA. Cancer J. Clin. vol. 69, no. 6, pp. 438–451, 2019.

[5] J Ma and A Jemal, *Breast Cancer Statistics*, in Breast Cancer Metastasis and Drug Resistance, A. Ahmad, Ed. New York, NY: Springer New York, 2013.

[6] S. H. Yun and S. J. J. Kwok, "Light in diagnosis, therapy and surgery," *Nat. Biomed. Eng.*, vol. 1, no. 1, pp. 1–16, 2017.

[7] M. J. C. Van Gemert and A. J. Welch, "Clinical use of laser-tissue interactions," IEEE Eng. Med. Biol. Mag. vol. 8, no. 4, pp. 10–13, 1989.

[8] M. H. Niemz, *Laser-tissue interactions*. Springer, 2007.

[9] M. D'Acunto, P. Cioni, E. Gabellieri, and G. Presciuttini, "Exploiting gold nanoparticles for diagnosis and cancer treatments," Nanotechnology, vol. 32, no. 19, pp. 192001, 2021.

[10] S. F. Karkan, M. Mohammad hosseini, Y. Panahi, M. Milani, N. Zarghami, A. Akbarzadeh, E. Abasi, A.Hosseini, and S. Davaran, "Magnetic nanoparticles in cancer diagnosis and treatment: a review," Artif. cells, nanomedicine, Biotechnol. vol. 45, no. 1, pp. 1–5, 2017.

[11] F. E. Rosa, R. M. Santos, S. R. Rogatto, and M. A. C. Domingues, "Chromogenic in situ hybridization compared with other approaches to evaluate HER2/neu status in breast carcinomas," Brazilian J. Med. Biol. Res., vol. 46, pp. 207–216, 2013.

[12] S. Badve and Y. Gökmen-Polar, *Molecular pathology of breast cancer*. Springer, 2016.

[13] A. Rasim Barutcu, B. R. Lajoie, R. P. McCord, C. E. Tye, D. Hong, T. L. Messier, G.Browne, A. J. van Wijnen, J. B. Lian, J. L. Stein, J. Dekker, A. N. Imbalzano, and G. S. Stein, "Chromatin interaction analysis reveals changes in small chromosome and telomere clustering between epithelial and breast cancer cells," Genome Biol. vol. 16, no. 1, pp. 1–14, 2015.

[14] M. Sheik-Bahae, A. A. Said, T.-H. Wei, D. J. Hagan, and E. W. Van Stryland, "Sensitive measurement of optical nonlinearities using a single beam," IEEE J. Quantum Electron. vol. 26, no. 4, pp. 760–769, 1990.

[15] S. L. Gómez, R. F. Turchiello, M. C. Jurado, P. Boschcov, M. Gidlund, and A. M. F. Neto, "Characterization of native and oxidized human low-density lipoproteins by the Z-scan technique.," Chem. Phys. Lipids, vol. 132, no. 2, pp. 185–195, 2004.

[16] S. L. Gómez, R. F. Turchiello, M. C. Jurado, P. Boschcov, M. Gidlund, and A. M. Figueiredo Neto, "Thermal-lens effect of low-density lipoprotein lyotropic-like aggregates investigated by using the Z-scan technique," Liq. Cryst. Today, vol. 15, no. 1, pp. 1–3, 2006.

[17] P. Dhinaa and A. Palanisamy, "Z-Scan technique: To measure the total protein and

albumin in blood," J. Biomed. Sci. Eng. vol. 3, pp. 285–290, 2010.

[18] A. N. Dhinaa and P. K. Palanisamy, "Optical nonlinearity in measurement of urea and uric acid in blood," Natural Science, Vol. 2, No.2, pp. 106- 111, 2010.

[19] A. Ghader, M. H. M. Ara, S. Mohajer, and A. Divsalar, "Investigation of nonlinear optical behavior of creatinine for measuring its concentration in blood plasma," Optik (Stuttg). vol. 158, pp. 231–236, 2018.

[20] A. Ghader, A. Abbasian Ardakani, H. Ghaznavi, A. Shakeri-Zadeh, S. Emamgholizadeh Minaei, S. Mohajer, and M. H. Majles Ara, "Evaluation of nonlinear optical differences between breast cancer cell lines SK-BR-3 and MCF-7; an in vitro study," Photodiagnosis Photodyn. Ther. vol. 23, pp. 171–175, 2018.

[21] B. Khaksar jalali, S.S. Mousavifard, S. Salmani shik, M.H. Majlesara, and M. Nabiuni, "The effect of gold nanoparticles on the optical properties of U87MG, brain cancer cells," opsi YR - pp. 697–700, 2019. [Online]. Available: http://opsi.ir/article-1-1915-fa.html

[22] S. S. Mousavifard, B. Khaksar jalali, S. Salmani shik, M. H. Majlesara, and M. Nabiuni, "The effect of gold nanoparticles on the linear and nonlinear behavior of malignant breast cancer of mda-mb-231 cell line," opsi YR - pp. 273–276, 2019. [Online]. Available: http://opsi.ir/article-1-1925-en.html

[23] A. Geltmeier, B. Rinner, D. Bade, K. Meditz, R. Witt, U. Bicker, C. Bludszuweit-Philipp, and P. Maier "Characterization of dynamic behaviour of MCF7 and MCF10A cells in ultrasonic field using modal and harmonic analyses," PLoS One, vol. 10, no. 8, pp. e0134999 (1-20), 2015.

[24] N. Caille, O. Thoumine, Y. Tardy, and J.-J. Meister, "Contribution of the nucleus to the mechanical properties of endothelial cells," J. Biomech. vol. 35, no. 2, pp. 177–187, 2002.

[25] "https://www.atcc.org/products/htb-22," 2022.

[26] "https://www.atcc.org/products/crl-10317," 2022.

[27] Y. Zhang, M. Yang, J.-H. Park, J. Singelyn, H. Ma, M. J. Sailor, E. Ruoslahti, M. Ozkan, and C. Ozkan "A Surface-Charge Study on Cellular-Uptake Behavior of F3-Peptide-Conjugated Iron Oxide Nanoparticles," Small, vol. 5, no. 17, pp. 1990–1996, 2009.

[28] G. Wypych, *Handbook of UV degradation and stabilization*. Elsevier, 2020.

[29] M. Hosseinzadeh, S. Salmani, M. H. Majles Ara, and S. Mohajer, "The simple optical methods for early diagnosis of selected benign and malignant brain tumors of human," J. Nonlinear Opt. Phys. Mater. vol. 27, no. 03, pp. 1850033, 2018.

[30] A. N. Dhinaa, A. Nooraldeen, K. Murali, and P. K. Palanisamy, "Z-scan technique as a tool for the measurement of blood glucose," Laser Phys. vol. 18, no. 10, pp. 1212–1216, 2008.

[31] S. Raji, M. A. Haddad, S. M. Moshtaghioun, and Z. Dehghan, "Nonlinear Optical Investigation of Biochemical Analytes in Blood Serum via Z-Scan Technique TT -," ssu-ijml, vol. 8, no. 4, pp. 291–303, 2021.

[32] R. W. Boyd, *The nonlinear optical susceptibility*, Elsevier, 2008.

[33] M. Sheik-Bahae, A. A. Said, and E. W. Van Stryland, "High-sensitivity, single-beam n 2 measurements," Opt. Lett. vol. 14, no. 17, pp. 955–957, 1989.

[34] Y. Qin, W. Jiang, A. Li, M. Gao, H. Liu, Y. Gao, X. Tian, and G. Gong, "The combination of paraformaldehyde and glutaraldehyde is a potential fixative for mitochondria," Biomolecules, vol. 11, no. 5, pp. 711, 2021.

[35] S.-O. Kim, J. Kim, T. Okajima, and N.-J. Cho, "Mechanical properties of paraformaldehyde-treated individual cells investigated by atomic force microscopy and scanning ion conductance microscopy," Nano Converg. vol. 4, no. 1, pp. 1–8, 2017.

[36] M. Salman, M. A. M. Hossein, K. S. Kamran, and M. Shayan, "Optical discrimination of benign and malignant oral tissue using Z-scan technique," Photodiagnosis Photodyn. Ther. vol. 16, pp. 54–59, 2016.

[37] K. J. Chalut and E. K. Paluch, "The Actin Cortex: A Bridge between Cell Shape and Function," Dev. Cell, vol. 38, no. 6, pp. 571–573, 2016.

[38] M. Salman, M. A. M. Hosein, and N. Mohammad, "Nonlinear optical investigation of normal ovarian cells of animal and cancerous ovarian cells of human in-vitro," Optik (Stuttg). vol. 127, no. 8, pp. 3867–3870, 2016.

[39] H. Abramczyk, J. Surmacki, M. Kopeć, A. K. Olejnik, K. Lubecka-Pietruszewska, and K. Fabianowska-Majewska, "The role of lipid droplets and adipocytes in cancer. Raman imaging of cell cultures: MCF10A, MCF7, and MDA-MB-231 compared to adipocytes in cancerous human breast tissue," Analyst, vol. 140, no. 7, pp. 2224–2235, 2015.